J. Fluid Mech. (1976), *vol.* 75, *part* 3, *pp.* 487–511
Printed in Great Britain

The hydrodynamic stability of rapidly evaporating liquids at reduced pressure

By HARVEY J. PALMER

Distillation Research Laboratory,
Rochester Institute of Technology, Rochester, New York 14614†

(Received 13 June 1975)

The hydrodynamic stability of a pure liquid undergoing steady rapid evaporation at reduced pressure is examined using linear stability analysis. Results show that the rapidly evaporating liquid is unstable to local variations in evaporation rate, local surface depressions being produced by the force exerted on the surface by the rapidly departing vapour and sustained liquid flows being driven by the resultant shear exerted on the liquid surface by the vapour. The coupling of this 'differential vapour recoil' mechanism to the Marangoni effect is investigated and the importance of inertial heat transfer, fluid inertia and viscous dissipation at the interface to system stability is resolved.

1. Introduction

Spontaneous convection in fluid–fluid systems driven by surface-tension variations and density stratification has been a subject of considerable interest in the past 20 years, for it is through such destabilizing mechanisms that the full utilization of otherwise stored potential energy can be accomplished. Numerous examples exist in which interfacial mass-transfer rates have been increased more than threefold by the onset of spontaneous convection (cf. Berg 1972; Beitel & Heideger 1971). Similar examples of heat-transport enhancement in fluid systems have also been reported.

In contrast, a third mechanism for inducing spontaneous convection, that of instability induced by differential vapour recoil, was first noted and correctly interpreted by Hickman in 1952 but has since attracted surprisingly little attention despite its dramatic effect on the evaporation of liquids at pressures below 1 Torr. Hickman (1952) has shown that an increase as high as 20-fold in the liquid evaporation rate may be enjoyed if the interface is disrupted by differential vapour recoil. The onset of such convection appears as a sharp transition from a relatively quiescent evaporating liquid surface as the pressure above the liquid is decreased. Consequently it is often responsible for spasmodic fluctuations in pressure during the operation of condensation pumps and vacuum distillation processes which can render the apparatus inoperative or ultimately result in complete loss of valuable product.

† Present address: Department of Chemical Engineering, University of Rochester, Rochester, New York 14627.

The influence of interfacial contamination on system behaviour is particularly important and has been qualitatively interpreted by Hickman (1952, 1972). Under certain circumstances the surface of the rapidly evaporating liquid separates into two distinct areas of interfacial activity (cf. figure 1, plate 1). Surface motion in the 'torpid' area reflects the slow bulk movement of the liquid below while the surface of the 'working' area exhibits rapid small-scale movement and a substantially increased evaporation rate. This large difference in the rates of evaporation from the two adjacent regions is reflected in the difference in their surface elevations ($\sim$ 2 mm), caused by the difference in momentum transfer to the surface by the departing vapour. The existence of the schizoid surface appears to be due solely to the presence of surface-active contamination in the system. In fact, by carefully overflowing the interfacial layer of the torpid area to discard any interfacial contaminants, Hickman has shown that the schizoid surface transforms to one which is entirely 'working'.

The object of the present paper is to assess the linear stability of a pure liquid undergoing steady rapid evaporation at reduced pressure. Included in the analysis are the effects of the discontinuities in both linear momentum and kinetic energy at the fluid–fluid interface which accompany the phase change. In addition, the relative importance of the ratio of convective to conductive heat transport to system stability is investigated and the coupling between the vapour recoil mechanism and the familiar surface-tension destabilizing mechanism (Marangoni instability) is assessed. A later paper will present the effects of trace amounts of non-volatile surfactants on the linear stability of rapidly evaporating liquids.

2. The quiescent system

Consider steady evaporation of a pure liquid at reduced pressure. The liquid is infinite in lateral extent and unbounded from below, and the rate of evaporation from the liquid surface is proportional to the local surface temperature:

$$\eta^* = E\left(\frac{M}{2\pi R}\right)^{\frac{1}{2}}\left[\frac{P^0}{T_{\mathrm{II}}^{*\frac{1}{2}}} - \frac{P_V^*}{T_V^{*\frac{1}{2}}}\right], \tag{1}$$

where η^* is the steady mass rate of evaporation, E is the evaporation coefficient, R is the gas constant, M is the molecular weight of the liquid, P^0 is its vapour pressure at the surface temperature T_{II}, and P_V^* and T_V^* are the pressure and temperature of the gas phase above the liquid (cf. Maa 1967).

Prior to the onset of interfacial instability, the surface temperature and evaporation rate are assumed to be independent of surface position. In general the bulk of the liquid will be circulating if not by mechanical agitation then by natural convection induced by density stratification. However, in the absence of instabilities driven by surface tension, a quiescent boundary layer may exist in the vicinity of the interface through which heat is transported by conduction only. The thickness of this boundary layer necessarily depends on the intensity of the bulk circulation. It is this interfacial region whose stability is to be analysed.

The evaporation rate is assumed to be steady. Thus there exists a net liquid flow upwards through the thermal boundary layer as well as a steady vapour flow away from the interface. Because of its relative insignificance and for simplicity, the effect of this liquid flow on the stable temperature profile in the thermal boundary layer is ignored in the present analysis. Therefore, prior to the onset of interfacial convection the temperature profile in the thermal boundary layer is assumed to be linear, consistent with the assumption of a steadily evaporating liquid, while the liquid temperature outside the boundary layer is assumed to be constant. The use of a 'broken-line' profile to characterize the temperature distribution in the liquid is not expected to restrict the applicability of the stability analysis (Brian & Ross 1972). This supposition is further supported by the close correspondence for long-wavelength disturbances between the present analysis and that of Miller (1973) for moving-boundary instabilities, which incorporated the exact initial temperature profile.

In addition, the rate of cooling of the liquid surface by heat conduction in the vapour phase is assumed to be negligible compared with the heat removed by the phase change. Furthermore, all physical properties of the two fluid phases except surface tension and vapour pressure are assumed constant. In particular, the destabilizing influence of an adverse density gradient in the boundary layer is ignored in the analysis. While density stratification should have a negligible effect on the stability of the thin thermal boundary layers (< 1 mm) exposed in Hickman's experiments, the buoyancy destabilizing mechanism (Rayleigh instability) will measurably decrease the stability of deeper layers and, therefore, must be reckoned with to provide accurate stability predictions for such systems.

Because mass must be conserved, the change in fluid density during evaporation results in a discontinuity in both the fluid velocity normal to the interface and the rate of transport of linear momentum across it. Momentum must also be conserved. Therefore the discontinuity in velocity results in a downward force on the interface (vapour recoil) which increases with evaporation rate and with an increase in the density ratio of the liquid and gas phase [cf. equation (3)]. Since the density of the gas phase is linearly proportional to the pressure, the magnitude and, thus, the importance of this vapour recoil force increase markedly as the pressure is reduced.

3. Destabilizing mechanisms

When the system is perturbed, it responds according to the equations of mass, momentum and energy conservation. Depending on the system properties, this response may carry it still further from the original unperturbed state. A disturbance in the form of a local increase in surface temperature, for example, will increase the local evaporation rate and decrease the local surface tension. The increase in evaporation rate produces a local increase in the normal force on the interface (vapour recoil). The result is a local depression or crater in the surface with slanted walls, which permits the departing vapour to shear the liquid surface and drag hot liquid up to the point of already higher temperature to

produce auto-amplification of the original disturbance. In a similar manner, the induced gradient in surface tension will induce the flow of hot liquid up to the surface to increase further the local surface temperature and amplify the disturbance.

Apart from the vapour-recoil and surface-tension mechanisms, fluid instability can also be produced by the effect of the deforming interface on the steady flow pattern near the surface. In the vicinity of surface depressions, fluid streamlines converge in the liquid phase and diverge in the vapour phase to reflect variations in fluid inertia, which produce a local decrease in liquid pressure combined with a local increase in vapour-phase pressure at the interface. The result is a net downward force, which depresses the surface still further. If the steady evaporation rate is sufficiently high, this inertia mechanism is capable of overcoming the stabilizing effect of gravity on surface deflexions to produce convection even in the absence of lateral variations in evaporation rate.

For disturbances of very short wavelength (i.e. less than one-tenth the thermal-boundary-layer thickness), the interconversion of viscous work and thermal energy becomes the major destabilizing factor in the system. Considerable point-wise variation in the slope of the interface accompanies any short-wavelength disturbance. Furthermore, high evaporation rates occur in the local surface depressions. Thus, in the vicinity of surface depressions fluid accelerations are high and viscous friction warms the surface liquid to sustain the locally high evaporation rate in the crater, while normal viscous forces further deform the interface.

If the wavelength of the disturbance is long (i.e. more than 1000 times the thermal-boundary-layer thickness), expansion during phase change coupled with convective heat transfer will aid in the auto-amplification of the disturbance. Local depressions in the interface cause local film thinning, which enhances heat transport to the surface, increases the local evaporation rate and, therefore, causes more rapid removal of liquid from depressions than from surface elevations to amplify the original disturbance. The interpretation of this moving-boundary destabilizing mechanism is given by Miller (1973), who examined the linear stability of a fluid–fluid interface during phase change subject to the restriction that the interfacial temperature remains constant while the local rate of phase transformation is perturbed. Compared with the present analysis, this special case refers to a liquid with an infinite temperature coefficient of evaporation rate. Thus Miller's analysis predicts a lower limit on the criteria for instability due to the moving-boundary mechanism in rapidly evaporating liquids. The present analysis expands Miller's results to encompass the more realistic condition of a liquid whose evaporation rate depends on interfacial temperature.

In summary, five distinct mechanisms for initiating interfacial convection in rapidly evaporating liquids will be delineated by the analysis: (i) differential vapour recoil, (ii) fluid inertia, (iii) viscous dissipation, (iv) moving boundary and (v) surface tension. Prior to execution of the formal stability analysis, certain qualitative trends in the stability criteria may be anticipated. The mechanisms of differential vapour recoil, fluid inertia and viscous dissipation

will all be accentuated by a decrease in gas-phase pressure. For the vapour-recoil mechanism, a decrease in pressure enhances crater formation through an increase in the magnitude of local variations in recoil force. For the fluid-inertia and viscous-dissipation mechanisms, a decrease in pressure intensifies the effect of fluid inertia on lateral pressure fluctuations at the interface and increases local viscous heating through an increase in gas-phase velocity and velocity gradients at constant mass evaporation rate.

If interfacial convection is to be induced by differential vapour recoil, by the fluid-inertia mechanism or by the viscous-dissipation mechanism, the interface must be deformable. Therefore a decrease in the surface tension will mean greater surface flexibility and a correspondingly greater propensity for convective instability. Furthermore, the existence of a vapour viscosity is essential if the departing vapour is to induce liquid flow by interfacial shear. Thus the larger the vapour viscosity the more unstable the system will be to differential vapour recoil. In contrast, the likelihood of instability induced by local variations in surface tension will be reduced by an increase in vapour viscosity because the induced interfacial shear stress must generate circulation in the vapour phase as well as in the liquid. In addition, while local increases in the evaporation rate at hot spots on the surface are crucial to the vapour-recoil mechanism to produce surface deformations, these local increases in evaporation rate also increase the local rate of interfacial cooling and diminish lateral temperature variations, which are vital to the surface-tension destabilizing mechanism. Thus some competition between the vapour-recoil mechanism and the surface-tension mechanism is anticipated in the following analysis. Finally, the action of gravity is to stabilize deflexions of the interface of moderate to long wavelength. Therefore gravitational stabilization will be significant to all but the viscous-dissipation destabilizing mechanism.

4. Mathematical formulation

The linear stability of the evaporating liquid is analysed in the usual manner by imparting to the quiescent system a small disturbance, exponential in time and periodic in the planform, spatial variables, but of arbitrary wavelength. The disturbance is then made to obey the conservation equations of mass, momentum and energy subject to the appropriate boundary conditions for the system.

The heart of the present analysis lies in the specification of the boundary conditions at the fluid interface. The general equations describing conservation of mass, momentum and energy in the interfacial region as presented by Slattery (1967) are simplified following Scriven & Sternling (1964) and Smith (1966) for an initially flat interface perturbed infinitesimally from its equilibrium position. The co-ordinate system used in this development moves with the unperturbed interface, with the z co-ordinate normal to the interface and increasing into the vapour phase.

For the quiescent system conservation of mass at the interface requires that

$$\rho_L W_L^* = \rho_V W_V^* = \eta^*, \tag{2}$$

where ρ is the mass density, W^* is the unperturbed vertical component of fluid velocity, η^* is the unperturbed mass rate of evaporation, and the subscripts L and V refer to the liquid and vapour phases respectively. The discontinuity in fluid velocity which accompanies the change in fluid density during phase change results in a discontinuity in the rate of transport of linear momentum across the fluid interface. The difference between the rate of momentum transport away from the interface by the departing vapour and the rate of momentum transport towards the interface by the approaching liquid is equal to a dynamic pressure $P_L^* - P_V^*$ exerted on the liquid surface, called the absolute vapour recoil force. The magnitude of this force is given by the following interfacial momentum balance:

$$P_L^* - P_V^* = \eta^{*2}(\rho_V^{-1} - \rho_L^{-1}), \tag{3}$$

where P^* is the unperturbed fluid pressure.

Finally, if heat conduction in the vapour phase is assumed to be negligible, the equation of energy conservation at the interface for the quiescent system becomes

$$\eta^* \lambda_{\text{vap}} + \tfrac{1}{2}\eta^{*3}(\rho_V^{-2} - \rho_L^{-2}) + k_L dT_L^*/dz = 0, \tag{4}$$

where λ_{vap} is the latent heat of vaporization for the fluid, k_L is the liquid thermal conductivity and T_L^* is the unperturbed liquid temperature.

If the system variables are now perturbed an infinitesimal amount from their quiescent values, conservation of mass at the interface requires that

$$\rho_L W_L' - \rho_V W_V' = (\rho_L - \rho_V) dB'/dt, \tag{5}$$

where B' is the displacement of the interface from its equilibrium position, t is time and the primes denote the perturbations in the system variables. In addition, it can be shown that there is a definite relationship between the perturbation in evaporation rate η' and the perturbation in the vertical component of velocity at the interface:

$$W_V' = \eta'/\rho_V + dB'/dt. \tag{6}$$

Continuity of tangential velocity at the interface results in the following boundary condition with the aid of the continuity equation:

$$\eta^* \left[\frac{1}{\rho_L} - \frac{1}{\rho_V}\right] \nabla_{\text{II}}^2 B' = \frac{\partial W_L'}{\partial z} - \frac{\partial W_V'}{\partial z}, \tag{7}$$

where ∇_{II}^2 is the surface divergence $\partial^2/\partial x^2 + \partial^2/\partial y^2$.

The requirement that momentum be conserved at the fluid interface results in both a normal and a tangential momentum balance at the interface for the perturbed system. The normal component of the interfacial momentum balance for this system is

$$(P_V' - P_L') + 2\eta^*\eta' \left[\frac{1}{\rho_V} - \frac{1}{\rho_L}\right] + 2\left[\mu_L \frac{\partial W_L'}{\partial z} - \mu_V \frac{\partial W_V'}{\partial z}\right] - \sigma^* \nabla_{\text{II}}^2 B' = 0, \tag{8}$$

where σ^* is the unperturbed value of the surface tension and μ is the fluid viscosity.

An equation representing the tangential component of the interfacial momen-

tum balance is obtained by taking the surface divergence of the interfacial momentum equation:

$$\nabla_{\mathrm{II}}^2\sigma' = \mu_L\left[\nabla_{\mathrm{II}}^2 W_L' - \frac{\partial^2 W_L'}{\partial z^2}\right] - \mu_V\left[\nabla_{\mathrm{II}}^2 W_V' - \frac{\partial^2 W_V'}{\partial z^2}\right], \tag{9}$$

where σ' is the perturbation in surface tension.

Finally, conservation of energy at the interface requires that

$$\eta'\lambda_{\mathrm{vap}} + k_L\frac{\partial T_L'}{\partial z} + \tfrac{3}{2}\eta'\eta^{*2}\left[\frac{1}{\rho_V^2} - \frac{1}{\rho_L^2}\right] - 2\eta^*\left[\frac{\mu_V}{\rho_V}\frac{\partial W_V'}{\partial z} - \frac{\mu_L}{\rho_L}\frac{\partial W_L'}{\partial z}\right] = 0. \tag{10}$$

Strictly, (5)–(10) are valid at the interface; i.e. at $z = B'$. For small surface deformations, however, it is easily shown that (5)–(7) remain unchanged if applied at $z = 0$. To modify (8) for application at $z = 0$, a Taylor series expansion of P' must be employed about $z = 0$. The result is that

$$[P_L' - P_V']_{z=B'} = [P_L' - P_V']_{z=0} - gB'(\rho_L - \rho_V), \tag{11}$$

where g is the gravitational acceleration.

Equations (9) and (10) may be similarly modified by recognizing that

$$[T_L']_{z=B'} = [T_L']_{z=0} - \beta B' \tag{12}$$

and that

$$\nabla_{\mathrm{II}}^2\sigma' = (\partial\sigma/\partial T)\,[\nabla_{\mathrm{II}}^2 T_L']_{z=B'}, \tag{13}$$

where $-\beta$ is the unperturbed temperature gradient in the thermal boundary layer and $\partial\sigma/\partial T$ is the temperature coefficient of surface tension.

The final form of the normal force balance applied at $z = 0$ is particularly interesting in that it reveals the distinguishing features of the destabilizing mechanisms in rapidly evaporating liquids. At $z = 0$

$$[P_V' - P_L'] + 2\eta^*\eta'\left[\frac{1}{\rho_V} - \frac{1}{\rho_L}\right] + 2\left[\mu_L\frac{\partial W_L'}{\partial z} - \mu_V\frac{\partial W_V'}{\partial z}\right] + g(\rho_L - \rho_V)B' - \sigma^*\nabla_{\mathrm{II}}^2 B' = 0, \tag{14}$$

where positive terms represent downward forces and negative terms represent upward forces. For a local depression $B' < 0$ while $\nabla_{\mathrm{II}}^2 B' > 0$. Thus the fourth and fifth terms of (14) are both negative and reveal the stabilizing effects of gravity and surface tension as restoring forces in the system. However, the first three terms in (14) are positive at local depressions of the interface owing to the associated increase in interfacial temperature and the local distortion of fluid streamlines. Thus these terms represent forces which tend to depress the interface still further and cause instability. In particular, the first term represents the destabilizing effect of local variations in bulk phase pressure caused by variations in fluid inertia, the second term is the destabilizing force of differential vapour recoil, and the third term reflects the destabilizing influence of normal viscous forces, which are important to the viscous-dissipation mechanism.

Far from the interface all perturbations in velocity and temperature must approach zero:

$$W'_L = \partial W'_L/\partial z = T'_L = 0 \quad \text{as} \quad z \to -\infty \tag{15}$$

and

$$W'_V = \partial W'_V/\partial z = 0 \qquad \text{as} \quad z \to \infty. \tag{16}$$

At the bottom boundary of the thermal boundary layer the liquid temperature T'_L and the heat flux $k_L \partial T'_L/\partial z$ must be continuous.

The linearized equations of mass, momentum and energy conservation together with the boundary conditions (5)–(10), (15) and (16) completely specify the response of the system to infinitesimal perturbations. The general form of the velocity, temperature and pressure disturbances which satisfies these equations is

$$\mathscr{P}'(x, y, z, t) = e^{\gamma t} f(x, y)\, \mathscr{P}(z),$$

where γ is the time growth constant, $\mathscr{P}(z)$ is the z-dependent part of the disturbance and $f(x, y)$ satisfies the two-dimensional wave equation

$$\nabla^2_{\mathrm{II}} f + \alpha^2 f = 0.$$

The state of marginal stability is sought and requires that the real part of the time growth constant be zero. In the present analysis only stationary modes of instability are considered. Therefore the imaginary part of γ is also set equal to zero. For the present system, the assumption of 'exchange of stabilities' appears to be justified since neither a non-conservative force field nor a superposed stabilizing gradient of solute or surfactant is present to favour oscillatory modes of instability (Veronis 1965; McConaghy & Finlayson 1969; Palmer & Berg 1972). After non-dimensionalization and requiring that $\gamma = 0$, the appropriate equations of momentum and energy conservation which define the neutrally stable state of the system become

$$(D^2 - \alpha^2) W_V - N_{RE} N_\mu D W_V - D P_V = 0, \tag{17}$$

$$(D^2 - \alpha^2) W_L - N_{RE} D W_L - D P_L = 0, \tag{18}$$

$$(D^2 - \alpha^2)(D^2 - \alpha^2 - N_{RE} N \mu D) W_V = 0, \tag{19}$$

$$(D^2 - \alpha^2)(D^2 - \alpha^2 - N_{RE} D) W_L = 0, \tag{20}$$

$$(D^2 - \alpha^2) P_V = 0, \quad (D^2 - \alpha^2) P_L = 0, \tag{21), (22}$$

$$(D^2 - \alpha^2 - N_{RE} N_{PR} D) T_L = \begin{cases} -W_L & \text{for} \quad -1 \leqslant \zeta \leqslant 0, \\ 0 & \text{for} \quad -\infty \leqslant \zeta \leqslant -1. \end{cases} \tag{23a, b}$$

Equations (17) and (18) are the equations of momentum conservation for each phase, (19) and (20) derive from the curl of the vorticity equation for each phase, (21) and (22) are the divergence of the equation of momentum conservation for each phase, and (23a, b) are those of energy conservation in the liquid.

Similarly the complete set of boundary conditions in dimensionless form is as follows. At $\zeta = 0$,

$$[N_{RE}N_{PR}N_{CR}(1-N_\rho^{-1})]\,W_V - N_H[T_L - B] = 0, \tag{24}$$

$$N_\rho W_L - N_\mu W_V = 0, \tag{25}$$

$$N_\mu DW_V - DW_L + N_{RE}N_{PR}(N_\rho - 1)\,\alpha^2 B = 0, \tag{26}$$

$$N_{CR}(P_L - P_V) + 2N_{CR}(DW_V - DW_L) - 2N_H(N_\mu/N_{PR})\,(T_L - B) - (\alpha^2 + N_{BO})\,B = 0, \tag{27}$$

$$\alpha^2 N_{MA}(T_L - B) + D^2 W_L - D^2 W_V + \alpha^2(W_L - W_V) = 0, \tag{28}$$

$$N_{PR}DT_L + W_L[1 + N_{BR}N_{RE}^2(N_\rho^2 - 1)]/N_{RE} + 2N_{BR}(DW_L - N_\rho DW_V) = 0. \tag{29}$$

As $\zeta \to \infty$, $W_V = DW_V = 0.$ (30), (31)

As $\zeta \to -\infty$, $W_L = DW_L = T_L = 0.$ (32)–(34)

At $\zeta = -1$, both T_L and DT_L must be continuous. (35), (36)

In (17)–(36), ζ is the dimensionless vertical co-ordinate; $D = d/d\zeta$; W, P and T are the ζ-dependent parts of the perturbations to the dimensionless vertical velocity component, pressure and temperature, respectively; B is the dimensionless amplitude of the interfacial displacement perturbation; and α is the wavenumber of the disturbance. The scaling factors for ζ, W_V, W_L, P_V, P_L, T_L and B are δ, $\kappa_L\mu_L/\mu_V\delta$, κ_L/δ, $\mu_L\kappa_L/\delta^2$, $\mu_L\kappa_L/\delta^2$, $\beta\delta$ and δ, respectively, where κ_L is the thermal diffusivity of the liquid and δ is the depth of the boundary layer.

The dimensionless groups in the above equations are defined as follows:

Hickman number $N_H = \left(\dfrac{\partial\eta}{\partial T}\right)\dfrac{\eta^*\beta\delta^2\mu_V}{\rho_L\kappa_L\sigma^*}\left(\dfrac{1}{\rho_V} - \dfrac{1}{\rho_L}\right)$,

Marangoni number $N_{MA} = -\left(\dfrac{\partial\sigma}{\partial T}\right)\dfrac{\beta\delta^2}{\kappa_L\mu_L}$,

Crispation number $N_{CR} = \mu_L\kappa_L/\sigma^*\delta$,

Viscosity ratio $N_\mu = \mu_L/\mu_V$,

Density ratio $N_\rho = \rho_L/\rho_V$,

Reynolds number $N_{RE} = \eta^*\delta/\mu_L$,

Prandtl number $N_{PR} = \nu_L/\kappa_L$,

Bond number $N_{BO} = \delta^2 g(\rho_L - \rho_V)/\sigma^*$,

Brinkman number $N_{BR} = \eta^*\nu_L^2/\beta k_L\delta^2$,

where ν is the kinematic viscosity and $\partial\eta/\partial T$ is the rate of change of evaporation rate with interfacial temperature.

Notice that both the Hickman number and the Marangoni number are functions of the thermal gradient $-\beta$ in the boundary layer and, consequently, are extremely useful for defining the stability limit for the system. In the absence of any variations in surface tension, the stability criteria are expressed in terms of the Hickman number, which is the ratio of the destabilizing forces of differential vapour recoil and vapour viscosity to the stabilizing action of surface tension and thermal diffusivity. Likewise, in the absence of lateral variations in evapora-

tion rate, the stability criteria for the system are expressed in terms of the Marangoni number, which is the ratio of the destabilizing surface forces to the stabilizing action of viscosity and thermal diffusivity.

It is important to recognize that the steady evaporation rate η^*, the heat of vaporization λ_{vap} and the steady liquid temperature gradient $-\beta$ are not mutually independent but are interrelated through the equation for conservation of energy at the interface for the quiescent system [cf. (4)]. Thus the Biot number, which represents the ratio of the rate of thermal energy transport at the surface by evaporative cooling to the rate of transport by conduction, does not appear in the present analysis.

5. General solution

The general solution to (19), (20) and (23*a*, *b*) which satisfies boundary conditions (30)–(34) is easily found to be

$$\begin{aligned}
W_V &= A_{11}e^{-\alpha\zeta} + A_{12}\exp(-r_V\zeta),\\
W_L &= A_{21}e^{\alpha\zeta} + A_{22}\exp(r_L\zeta),\\
T_L &= A_{31}e^{q\zeta} + A_{32}\exp[(N_{RE}N_{PR}-q)\zeta] + A_{21}e^{\alpha\zeta}/(\alpha N_{RE}N_{PR})\\
&\quad + A_{22}\exp(r_L\zeta)/[r_L N_{RE}(N_{PR}-1)] \quad \text{for} \quad \zeta \geqslant -1,\\
T_L &= A_{33}e^{q\zeta} \text{ for } \quad \zeta < -1,
\end{aligned}$$

where

$$\begin{aligned}
r_V &= \tfrac{1}{2}[-N_{RE}N_\mu + (N_{RE}^2N_\mu^2 + 4\alpha^2)^{\frac{1}{2}}],\\
r_L &= \tfrac{1}{2}[N_{RE} + (N_{RE}^2 + 4\alpha^2)^{\frac{1}{2}}]
\end{aligned}$$

and

$$q = \tfrac{1}{2}[N_{RE}N_{PR} + (N_{RE}^2N_{PR}^2 + 4\alpha^2)^{\frac{1}{2}}].$$

The relationships between the integration constants A_{ij} may be determined from boundary conditions (24)–(27), (29), (35) and (36) with the aid of (17), (18), (21) and (22) following Scriven & Sternling (1964). Substitution of the results into the shear-stress balance at the interface [equation (28)] then yields the following characteristic equation relating the Hickman number to α and the other dimensionless groups at the condition of neutral stationary instability:

$$N_H = [N_{RE}^2N_{PR}^2N_{CR}(N_\rho - 1)/N_\mu]\left[\frac{\alpha q\lambda_1}{N_\rho\lambda_2} - \frac{\alpha(\alpha - r_V)\lambda_3 N_{MA}}{\lambda_2 N_{RE}N_{PR}}\right], \tag{37}$$

where

$$\begin{aligned}
\lambda_1 &= (r_L - r_V)(N_\mu/N_\rho)(\alpha^2 + N_{BO})/(\alpha N_{RE}N_{PR}N_{CR})\\
&\quad + N_{RE}N_\mu(1 - N_\rho^{-1})[r_V(r_L - \alpha)/(r_L + \alpha) - r_L(\alpha - r_V)/(\alpha + r_V)],\\
\lambda_2 &= \lambda_3[N_{RE}(r_L + N_\rho r_V) + 2\alpha(\alpha - r_V)(1 - N_\rho/N_\mu)]\\
&\quad + [N_\rho - 2 + (r_L + \alpha N_\rho)/(\alpha - r_V) + 2r_L(1 - N_\mu^{-1})/N_{RE}][r_V N_{RE}N_\mu(1 - N_\rho^{-1})\\
&\quad \times (\lambda_4 - \lambda_5) + (N_{RE}/N_\rho)(r_L - r_V)(2\alpha^2 N_{RE}N_{BR}(N_\rho - 1) + qN_\mu/N_\rho)]\\
&\quad + \lambda_1[\lambda_5 - \alpha/N_\rho - \alpha N_{RE}^2 N_{BR}(N_\rho^2 - 1)/N_\rho],\\
\lambda_3 &= (\lambda_4 - \lambda_5)[(N_\mu/N_\rho)(\alpha^2 + N_{BO})/(\alpha N_{RE}^2 N_{PR}N_{CR}) - \alpha N_\mu(1 - N_\rho^{-1})/(\alpha + r_V)]\\
&\quad - N_\rho^{-1}(r_L - \alpha)[(\alpha + r_V)^{-1} + (\alpha + r_L)^{-1}][2\alpha^2 N_{RE}N_{BR}(N_\rho - 1) + qN_\mu/N_\rho],\\
\lambda_4 &= N_\rho^{-1}(q - \alpha)[1 - \exp(N_{RE}N_{PR} - \alpha - q)] + 2\alpha^2 N_{RE}N_{BR}(N_\rho - N_\mu)/N_\rho N_\mu,\\
\lambda_5 &= \{\alpha N_{PR}(q - r_L)/[r_L N_\rho(N_{PR} - 1)]\}\{1 - \exp(N_{RE}N_{PR} - r_L - q)\}\\
&\quad + 2\alpha r_L N_{RE}N_{BR}(N_\rho - N_\mu)/N_\rho N_\mu.
\end{aligned}$$

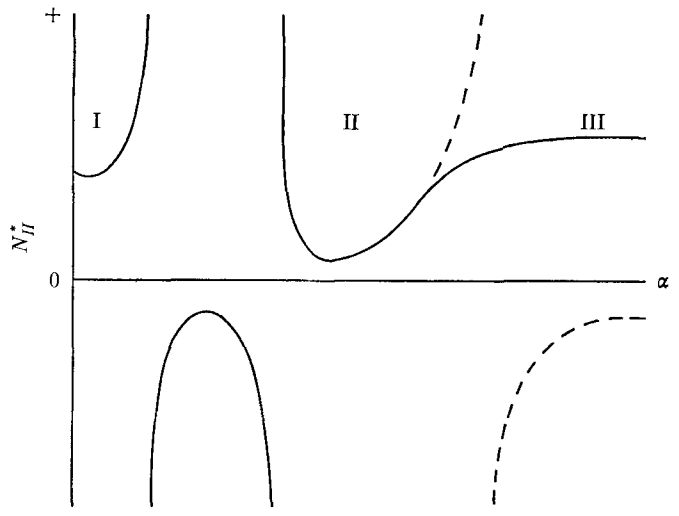

FIGURE 2. Typical behaviour of the critical Hickman number with wavenumber. Region I is due to the moving-boundary mechanism, region II to vapour recoil and region III to viscous dissipation. – – –, $N_{BR} = 0$.

In §6 the stability criteria for rapidly evaporating liquids in the absence of destabilizing surface-tension gradients will be discussed. In §7 the coupling between the surface-tension mechanism and the vapour-recoil mechanism is explored and the theoretical predictions are interpreted in the light of the available experimental data.

6. Instability in the absence of surface-tension gradients

6.1. *Wavenumber dependence*

In the absence of local variations in surface tension, $N_{MA} = 0$ and the condition of marginal stability is expressed in terms of the Hickman number, denoted by N_H^*. For this case four independent destabilizing mechanisms are potentially operative in rapidly evaporating liquids. For disturbances of moderate wavelength ($\alpha \to 1$), instabilities driven by differential vapour recoil and by the fluid-inertia mechanism are favoured; for disturbances of very small wavelength ($\alpha \to \infty$), auto-amplification occurs via the viscous-dissipation mechanism; while for long-wavelength disturbances ($\alpha \sim 10^{-3}$), instability may be produced by the moving-boundary mechanism.

Because of the substantial differences in preferred wavelength for each mechanism, there is essentially no reinforcement of either the viscous-dissipation mechanism or the moving-boundary mechanism by differential vapour recoil or by local variations in fluid inertia. Thus criteria for instability induced by viscous dissipation or by the moving-boundary mechanism are easily deduced by limiting perspective to the appropriate range of wavenumbers.

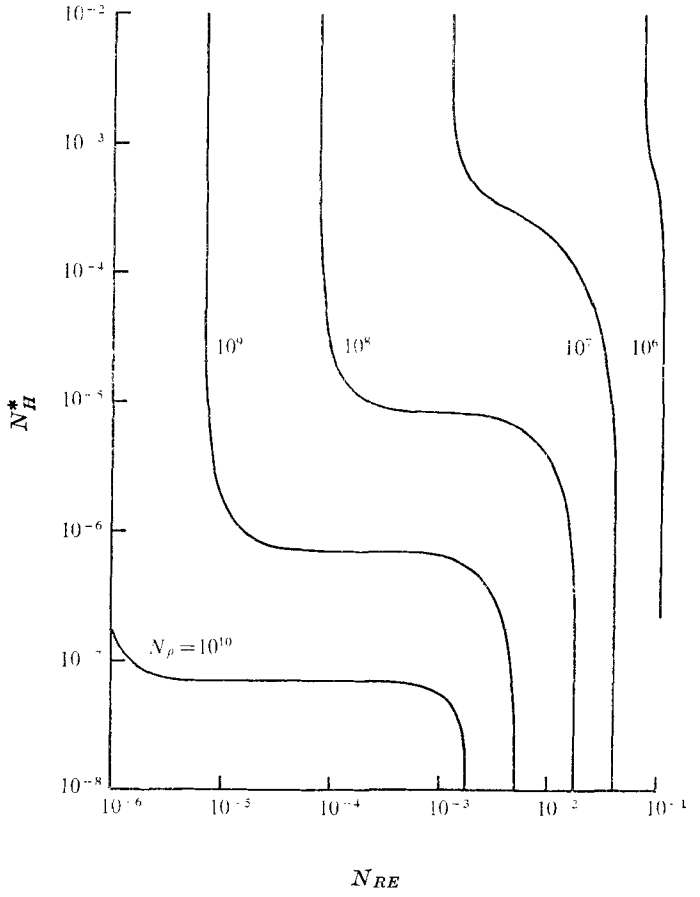

FIGURE 3. The dependence of the critical Hickman number on liquid-phase Reynolds number for the case in which the mechanism of differential vapour recoil dominates. $N_{CR} = 10^{-5}$, $N_{BO} = 1$, $N_{PR} = 10$, $N_\mu = 10^2$, $N_{BR} = 0$, $N_{MA} = 0$.

The exclusiveness of these two mechanisms is easily visualized with the aid of figure 2, which schematically illustrates the typical behaviour of N_H^* with wavenumber. Because negative values of the Hickman number are physically unrealistic, only neutral-stability curves for positive N_H^* are of interest. Region I is the region of instability due to the moving-boundary mechanism, region II is that due to the combined effects of differential vapour recoil and fluid inertia, and region III is that due to the viscous-dissipation mechanism, while the dashed line indicates the shape of the neutral-stability curve if the effect of viscous dissipation is eliminated by setting $N_{BR} = 0$. Naturally the relative location of the minima and the asymptote at $\alpha \to \infty$ will depend on the values of the pertinent dimensionless groups. For instance, if viscous dissipation dominates the vapour-recoil mechanism, the value of N_H^* as $\alpha \to \infty$ will also be the minimum in the solid curve II–III. Similarly, if the minimum in curve I is less than the minimum in curve II–III, then the moving-boundary mechanism will initiate convective

instability (assuming that such long-wavelength disturbances can enter the system).

In contrast to the simplicity of isolating the viscous-dissipation and moving-boundary mechanisms, the destabilizing effect of differential vapour recoil in the absence of the effects of fluid inertia can be revealed only if the inertial terms of the equation of motion are ignored. Since little is gained by introducing this artificial restriction, the criteria for instability induced by differential vapour recoil will be presented with reinforcement by fluid inertia implicit in the results. The limiting case of N_H^* equal to zero will then be explored to reveal the potential for instability via the fluid-inertia mechanism only.

6.2. *Instability induced by differential vapour recoil*

By far the most important mechanism for producing interfacial convection in rapidly evaporating liquids at reduced pressure is differential vapour recoil. As will be demonstrated in § 7, application of the present theory to the evaporation under vacuum of real fluids from a horizontal interface predicts instability via the vapour-recoil mechanism and qualitative experimental observations seem to bear this out.

The criteria for instability induced by differential vapour recoil are presented in terms of the critical Hickman number N_H^*, which is the minimum in curve II of figure 2 for $N_{BR} = 0$. The dependence of N_H^* on the liquid-phase Reynolds number N_{RE} is illustrated in figure 3. Notice that for each value of the liquid-to-vapour density ratio N_ρ there is a value of the Reynolds number below which N_H^* is infinite. This critical value of N_{RE} must be surpassed before instability by the vapour-recoil mechanism is possible. In other words, the *absolute* recoil force must exceed a critical value before local *variations* in recoil force will be capable of producing an auto-amplifying disturbance. Beyond the critical value of N_{RE}, however, the critical Hickman number remains essentially independent of Reynolds number until inertial forces become so great that they are capable of producing instability even in the absence of local variations in evaporation rate (as indicated by the sharp decrease in N_H^* to zero at high values of N_{RE}). Notice also that, as the liquid-to-vapour density ratio is increased, the range of N_{RE} in which instability induced by differential vapour recoil is possible broadens and that the value of N_H^* within this region decreases in proportion to the increase in N_ρ. An increase in N_ρ produces an increase in the velocity of the vapour leaving the surface, thereby increasing the shearing force on the liquid and decreasing system stability.

Similarly shaped curves are shown in figure 4, in which the effect of surface flexibility on system stability is illustrated. As the crispation number N_{CR} increases, the interface becomes more deformable and smaller evaporation rates (and thus smaller values of N_{RE}) are required to produce instability induced by differential vapour recoil. The major effect of the crispation number for $N_{CR} \geqslant 10^{-5}$ is to shift the range of Reynolds numbers for which instability induced by differential vapour recoil is plausible. The crispation number has little influence on the actual stability criteria within this region. However, for $N_{CR} < 10^{-5}$ this range of N_{RE} begins to narrow drastically until, at $N_{CR} = 10^{-7}$,

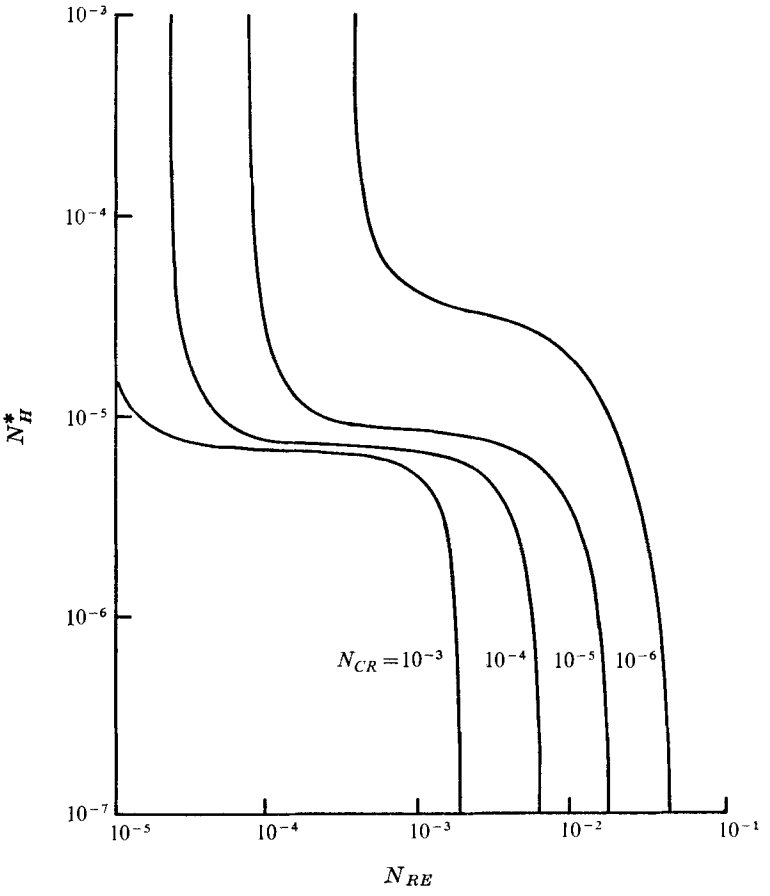

FIGURE 4. The effect of surface flexibility (in terms of N_{CR}) on the critical Hickman number for instability induced by differential vapour recoil. $N_{BO} = 1$, $N_{PR} = 10$, $N_\rho = 10^8$, $N_\mu = 10^2$, $N_{BR} = 0$, $N_{MA} = 0$.

the propensity for instability induced by differential vapour recoil is essentially non-existent. This situation represents an interface which is sufficiently non-deformable to prevent any formation of interfacial craters by local variations in evaporation rate and the resultant shearing of the liquid by the vapour which is necessary for this mechanism to produce convection.

The effect of Prandtl number on the curve of N_H^* *vs.* N_{RE} is identical to that of the crispation number. As N_{PR} increases, convective heat transport becomes an increasingly more dominant destabilizing influence for maintaining lateral variations in interfacial temperature. Therefore the Reynolds number necessary for instability gradually decreases. As in the case of the crispation number, however, the Prandtl number has little effect on the value of N_H^* within the region of potential instability induced by differential vapour recoil.

Crucial to the mechanism of differential vapour recoil is the existence of vapour viscosity. The effect of the liquid-to-vapour viscosity ratio on the stability limit for the system is presented in figure 5. Because vapour viscosity at

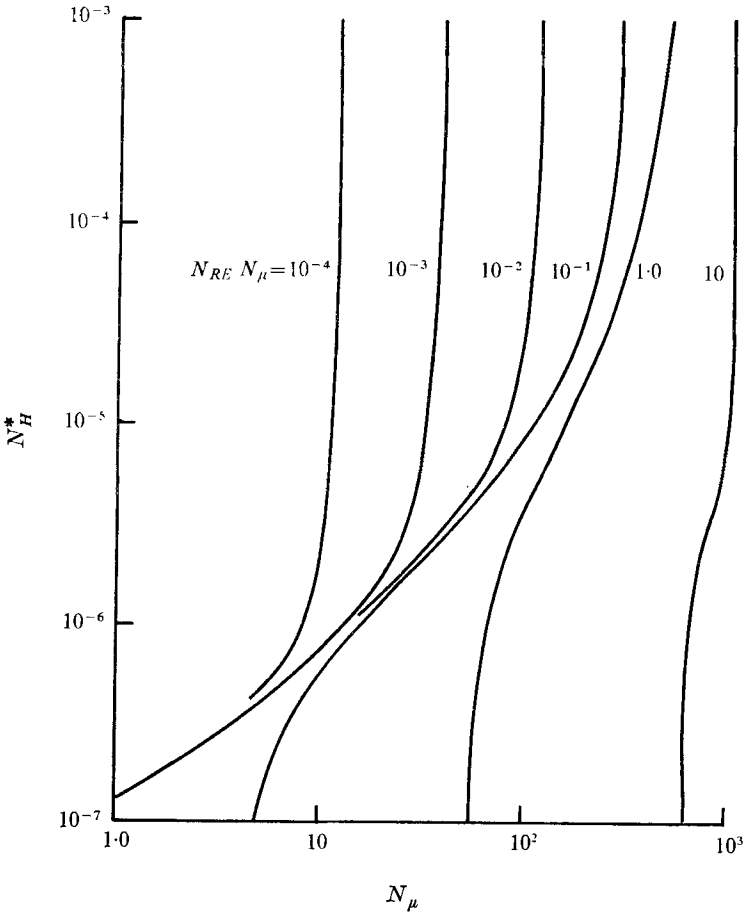

FIGURE 5. The dependence of the critical Hickman number on the liquid-to-vapour viscosity ratio at constant vapour-phase Reynolds number for the case of instability induced by differential vapour recoil. $N_{CR} = 10^{-5}$, $N_{BO} = 1$, $N_{PR} = 10$, $N_\rho = 10^8$, $N_{BR} = 0$, $N_{MA} = 0$.

a fixed temperature and sub-atmospheric pressure is relatively independent of the particular fluid considered, curves of constant vapour-phase Reynolds number $N_{RE}N_\mu$ are most useful in evaluating the effect of viscosity ratio on system stability. As expected, the critical Hickman number decreases in proportion to a decrease in N_μ in the region of potential instability by the vapour-recoil mechanism. Also, for a fixed value of $N_{RE}N_\mu$, there is a critical value of the liquid-to-vapour viscosity ratio above which vapour shearing of the interface is incapable of inducing convection in the fluid regardless of the value of N_H^*.

The degree of gravitational stabilization of long-wavelength disturbances is proportional to the Bond number N_{BO}. Consequently, as the Bond number is increased the critical wavenumber, corresponding to the minimum in the neutral-stability curve of N_H^* *vs.* α, is shifted to higher and higher wavenumbers

(smaller and smaller wavelengths). For example, for typical values of all the other dimensionless groups ($N_{CR} = 10^{-5}$, $N_{PR} = 10$, $N_{RE} = 10^4$, $N_\rho = 10^8$, $N_\mu = 10^2$, $N_{BR} = 0$ and $N_{MA} = 0$), the critical Hickman number occurs at $\alpha = 1{\cdot}5$ for $N_{BO} = 1{\cdot}0$ and at $\alpha = 0{\cdot}2$ for $N_{BO} = 10^{-2}$. Thus, for a boundary layer 1 mm thick, the critical convection cell size will be approximately 4 and 30 mm for $N_{BO} = 1{\cdot}0$ and 10^{-2}, respectively. The effect of the Bond number on the critical Hickman number is presented in figure 6. Because the vapour-recoil mechanism amplifies disturbances of moderate wavelength and because gravitational stabilization is most important for disturbances of long wavelength, the effect of low values of the Bond number on the criteria for instability is negligible. However, as the Bond number increases above 0·1, gravitational stabilization becomes increasingly important at moderate wavelengths and the critical Hickman number begins to increase markedly. Notice also that, if the Reynolds number is sufficiently high ($> 10^{-2}$ in this case) and the Bond number is sufficiently low ($< 10^{-1}$), instability due to fluctuations in fluid inertia is possible.

In summary, the potential for instability induced by differential vapour recoil exists over a narrow range of Reynolds numbers whose span is determined by the values of the various dimensionless groups of the system. The value of the critical Hickman number within this range of Reynolds numbers is most sensitive to N_ρ and N_μ and least sensitive to N_{CR}, N_{BO} and N_{PR}.

6.3. *The fluid-inertia destabilizing mechanism*

In the absence of any variation in evaporation rate, instability at moderate wavelengths is due entirely to local variations in fluid inertia which accompany local deflexions of the interface. For this special case the stability limit is the condition for which $\lambda_1 = 0$ and is best described in terms of N_I, which proves to be a function of N_{BO}, N_{RE} and N_μ according to the following equation:

$$N_I = \frac{(r_L - r_V)(\alpha + N_{BO}/\alpha)}{r_L(\alpha - r_V)/(\alpha + r_V) - r_V(r_L - \alpha)/(r_L + \alpha)}, \tag{38}$$

where the inertial number N_I is defined by the equation

$$N_I = N_{RE}^2 N_{PR} N_{CR}(N_\rho - 1) = \frac{\eta^{*2}\delta}{\sigma^*}\left[\frac{1}{\rho_V} - \frac{1}{\rho_L}\right].$$

Figure 7 illustrates the weak dependence of the critical inertial number on both the vapour-phase Reynolds number $N_{RE}N_\mu$ and the viscosity ratio for the realistic situation $N_\mu > 10$. Because of this weak dependence of N_I on N_μ for systems of practical interest, the general criteria for instability induced by local variations in fluid inertia may be presented on a single graph of critical inertial number *vs.* Bond number as shown in figure 8. Notice that for these circumstances $N_I = \epsilon N_{BO}^{\frac{1}{2}}$, where the proportionality constant ϵ is a weak function of the vapour-phase Reynolds number and varies between two and four. Consequently, for rapidly evaporating liquids instability is guaranteed if

$$\frac{N_I}{N_{BO}^{\frac{1}{2}}} = \frac{\eta^{*2}}{\rho_L \rho_V}\left[\frac{\rho_L - \rho_V}{\sigma^* g}\right]^{\frac{1}{2}} > 4. \tag{39}$$

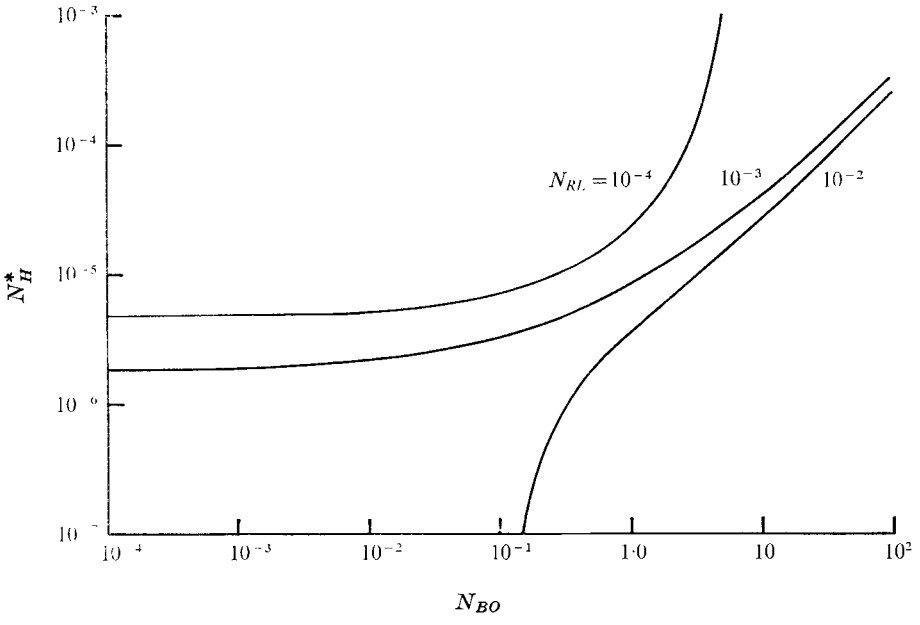

FIGURE 6. The effect of Bond number on the potential for instability induced by differential vapour recoil. $N_{CR} = 10^{-5}$, $N_{PR} = 10$, $N_\rho = 10^8$, $N_\mu = 10^2$, $N_{BR} = 0$, $N_{MA} = 0$.

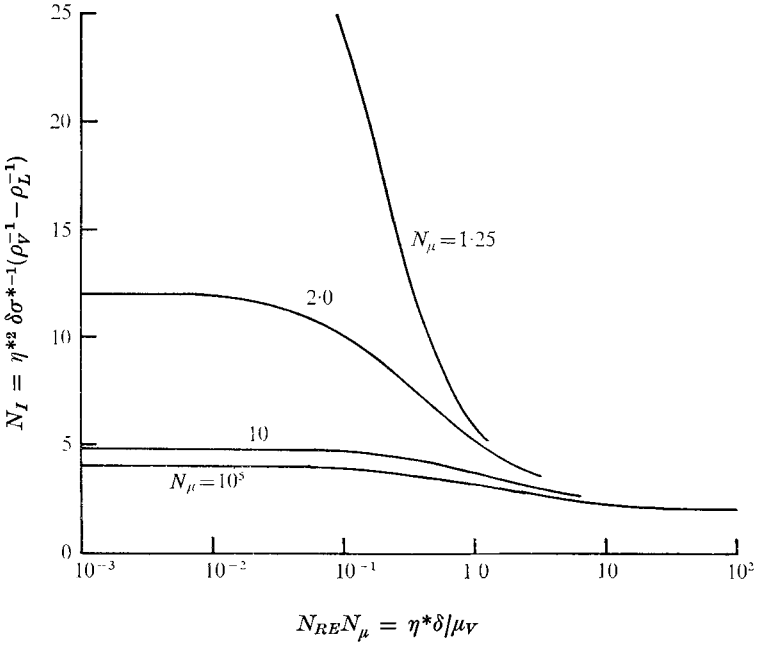

FIGURE 7. The effect of vapour-phase Reynolds number and liquid-to-vapour viscosity ratio on the criteria for instability induced by local variations in fluid inertia at the interface; $N_{BO} = 1$.

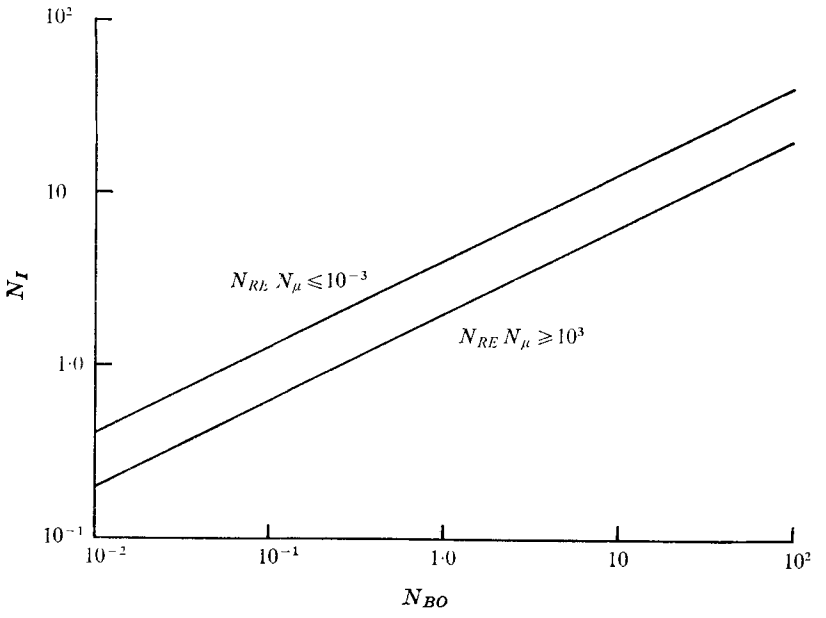

FIGURE 8. The criteria for instability due to the fluid-inertia mechanism as a function of Bond number for $N_\mu > 10$.

At reduced pressures, this criterion is not difficult to attain. On the contrary, evaporation rates of 10^{-3} g/cm^2 s are common, which means that a pressure of 10^{-3} Torr is sufficiently low to produce instabilities induced by fluid inertia.

Because the potential for instability induced by fluid inertia increases as the gravitational force normal to the interface decreases as reflected in (39), the system becomes more unstable as the interface is inclined to the horizontal. On the other hand, the stability limit for instability induced by differential vapour recoil is insensitive to a decrease in the gravity force normal to the interface for small values of N_{BO} (cf. figure 6). Therefore, while differential vapour recoil is the significant mechanism for producing instabilities at horizontal interfaces, the fluid-inertia mechanism dominates in rapidly evaporating liquids on steeply inclined surfaces and, possibly, in nucleate boiling processes.

6.4. *Instability induced by viscous dissipation*

For disturbances of very small wavelength ($\alpha > 10^3$), the lateral variations in viscous dissipation that accompany local deflexions of the interface are capable of generating enough heat to sustain locally higher evaporation rates in surface craters and, therefore, to cause instability. As illustrated in figure 2, the curve of N_H^* *vs.* α asymptotically approaches a limiting value at large α. This limit represents the critical Hickman number for instability induced by viscous dissipation. Thus the criteria for instability induced by the viscous-dissipation mechanism are easily determined by taking the limit of (37) as α approaches infinity. The result is

$$[N_H^*]_{\alpha\to\infty} = N_{PR}(1+N_\mu)/[4N_{BR}(N_\rho+1)\,(N_\mu+N_\rho)], \tag{40}$$

or in modified form

$$\bar{N}_H^* = \frac{(1+N_\mu^{-1})}{4(1+N_\mu/N_\rho)(1-N_\rho^{-2})}, \tag{41}$$

where $\bar{N}_H^*$ is a modified Hickman number defined by

$$\bar{N}_H^* = N_H^* N_{BR} N_\rho^3/[N_\mu N_{PR}(N_\rho - 1)] = \left(\frac{\partial\eta}{\partial T}\right)\frac{\eta^{*2}\mu_V^2}{\rho_V^3 \sigma^* k_L}. \tag{42}$$

For vapour–liquid systems at low pressures N_μ^{-1}, N_μ/N_ρ and N_ρ^{-2} are much less than unity. Therefore, the criterion for instability due to viscous dissipation reduces to $\bar{N}_H^* > \frac{1}{4}$. Because $\bar{N}_H^*$ is proportional to ρ_V^{-3}, the criterion for instability may be exceeded for vaporization at reduced pressure. In fact, for a typical value of η^* of 2×10^{-3} g/cm^2 s, a vacuum of 10^{-2} Torr is sufficient to produce instability induced by viscous dissipation in most circumstances.

Equation (42) reveals the insignificance of the thermal gradient and the boundary-layer thickness for instability induced by the viscous-dissipation mechanism. Thus it is expected that the viscous-dissipation destabilizing mechanism will be most important in systems with very thin thermal boundary layers, possibly resulting from rapid agitation in the bulk phase, for which the criteria for instability induced by differential vapour recoil are not exceeded.

6.5. *The moving-boundary mechanism*

For disturbances of very long wavelength ($\alpha \to 0$), auto-amplification may occur owing to the moving-boundary mechanism described by Miller (1973). Although the minimum in the curve of N_H^* *vs.* α in region I of figure 2 does not occur at $\alpha = 0$, the neutral-stability curve is extremely flat in the region $0 < \alpha < 10^{-3}$ within which the minimum value of N_H^* falls. Therefore, the limiting value of N_H^* as $\alpha \to 0$ is generally within 1% of the minimum criterion for instability induced by the moving-boundary mechanism. As the wavenumber approaches zero,

$$\frac{N_\mu[N_H^*]_{\alpha\to 0}}{N_{RE}^2 N_{PR}^2 N_{CR}(N_\rho - 1)} = \left\{1 + \frac{2N_{RE}^2 N_{PR} N_{CR} N_\rho}{N_{BO}} - \frac{1 + N_{BR} N_{RE}^2 (N_\rho^2 - 1)}{N_{RE} N_{PR}}\right\}^{-1}. \tag{43}$$

The second term on the right-hand side of (43) represents the destabilizing effect of surface flexibility while the third term represents the stabilizing effect of interfacial cooling by vaporization plus conversion of heat to kinetic energy of the emerging vapour. For most circumstances, interconversion of thermal energy to kinetic energy is unimportant and, therefore, the effect of the term containing N_{BR} may be ignored. For such situations stability is guaranteed if $N_{RE} N_{PR}$ is greater than unity. This simple 'rule of thumb' proves to be a convenient indicator of whether the moving-boundary mechanism is capable of producing an instability in a particular system of interest.

If N_{BR} is assumed equal to zero and (43) is rewritten in terms of system properties as

$$\left(\frac{\partial\eta}{\partial T}\right)\frac{\beta d}{\eta^*} = \left\{1 + \frac{2\eta^{*2}}{\rho_V g\delta(\rho_L - \rho_V)} - \frac{\rho_L \kappa_L}{\eta^* \delta}\right\}^{-1}, \tag{44}$$

the stability limit for instability via the moving-boundary mechanism is seen to be independent of liquid viscosity. This is because the moving-boundary mechanism produces instabilities in the form of interfacial wave amplification rather than as interfacial convection.

The above result differs from that of Miller (1973) in that it allows for the stabilizing effect of the dependence of evaporation rate on local interfacial temperature. Because Miller assumed that the evaporation rate can vary while the surface temperature remains constant, his stability criteria are based on the assumption that N_H is infinite. In reality, however, this is never the case. Therefore his results represent a lower bound on the criteria for instability predicted from (44). Nevertheless, his conclusion that instability can exist only for disturbances of (impermissibly) long wavelength remains unchanged. In addition, computations based on physical properties of real systems indicate that instability due to differential vapour recoil, fluid inertia or viscous dissipation is far more likely than that due to the moving-boundary mechanism.

7. General solution including the effect of surface-tension gradients

Before exploring the degree of interaction between the preceding destabilizing mechanisms and the surface-tension destabilizing mechanism, the effect of the various dimensionless groups on the critical Marangoni number N^*_{MA} in the absence of local variations in evaporation rate must be assessed by setting $N_H = 0$ in (37). The results indicate that N^*_{MA} is highly insensitive to N_{PR}, N_{CR}, N_{BO}, N_μ, N_ρ and N_{BR} for realistic values of these dimensionless groups while the major effect of the Reynolds number is to shift the critical wavenumber to higher and higher values as N_{RE} increases, as shown in table 1.

In §3 it was explained that local variations in evaporation rate diminish lateral variations in surface temperature to stabilize instability driven by surface tension. This stabilizing effect may be isolated from the destabilizing effect of differential vapour recoil by computing the critical Marangoni number N_{MA} as a function of N_H/N_{MA} under conditions for which instability due to vapour recoil is impossible. The result of these calculations is presented in figure 9. Notice that, as the effect of local variations in evaporation rate is increased relative to that of surface-tension gradients, the critical Marangoni number increases sharply and ultimately approaches infinity. This dramatic increase in stability is accompanied by only a small decrease in preferred disturbance wavelength, which supports the contention that the significant stabilizing effect is due to local interfacial cooling and not to a change in the stabilizing influence of fluid viscosity with wavenumber.

The effect of surface-tension gradients on instability produced by the viscous-dissipation, fluid-inertia and moving-boundary mechanisms is negligible. However, because of their similarity in requiring interfacial shearing of the liquid to induce convection and amplify disturbances, the interaction between the surface-tension mechanism and the mechanism of differential vapour recoil can be considerable. To expose this interaction between these two destabilizing mechanisms, the stability criteria for systems in which both mechanisms are

N_{RE}	$N_{MA}{}^*$	α
0	4·010	0
10^{-5}	4·107	0·0063
10^{-4}	4·253	0·020
10^{-3}	4·747	0·063
10^{-2}	6·604	0·20

TABLE 1. The effect of Reynolds number on the criteria for instability driven by surface tension. $N_{PR} = 10$, $N_\rho = 10^3$, $N_\mu = 10^2$, $N_{BO} = 1$, $N_{CR} = 10^{-5}$, $N_{BR} = 0$.

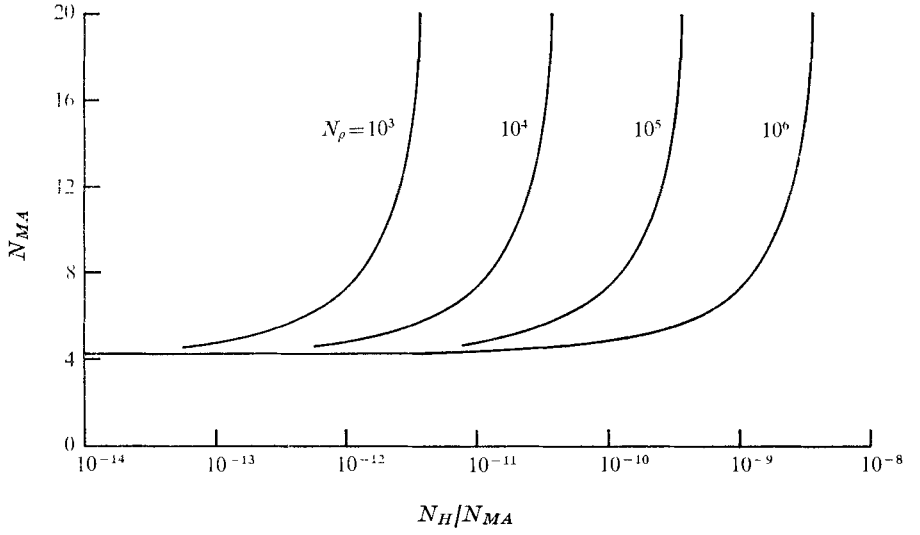

FIGURE 9. The effect of Hickman number on the criteria for instability driven by surface tension under conditions for which all other destabilizing mechanisms are inoperative. $N_{PR} = 10$, $N_{CR} = 10^{-5}$, $N_{BO} = 1$, $N_\mu = 10^2$, $N_{RE} = 10^{-4}$, $N_{BR} = 0$.

operative are presented as a normalized critical Marangoni number N_{MA}/N^*_{MA} *vs.* a normalized critical Hickman number N_H/N^*_H. Figures 10(*a*) and (*b*) show the normalized critical Marangoni number *vs.* the normalized critical Hickman number for the range of N_ρ in which the destabilizing mechanism of differential vapour recoil is operative for Bond numbers of 1·0 and 10^{-2} respectively.

Unlike the case of instability driven by the combined effects of surface tension and buoyancy investigated by Nield (1964), there is surprisingly little coupling between the destabilizing mechanism of differential vapour recoil and that due to gradients in surface tension. In fact, over most of the range of N_ρ for which both mechanisms are operative, there is actually an increase in system stability followed by a decrease as the Hickman number is increased. Thus, as the evaporation rate is increased (to increase the effect of vapour recoil) the system may first exhibit convection driven by surface tension, then become stable, and finally become unstable again owing to the effect of differential vapour recoil. This

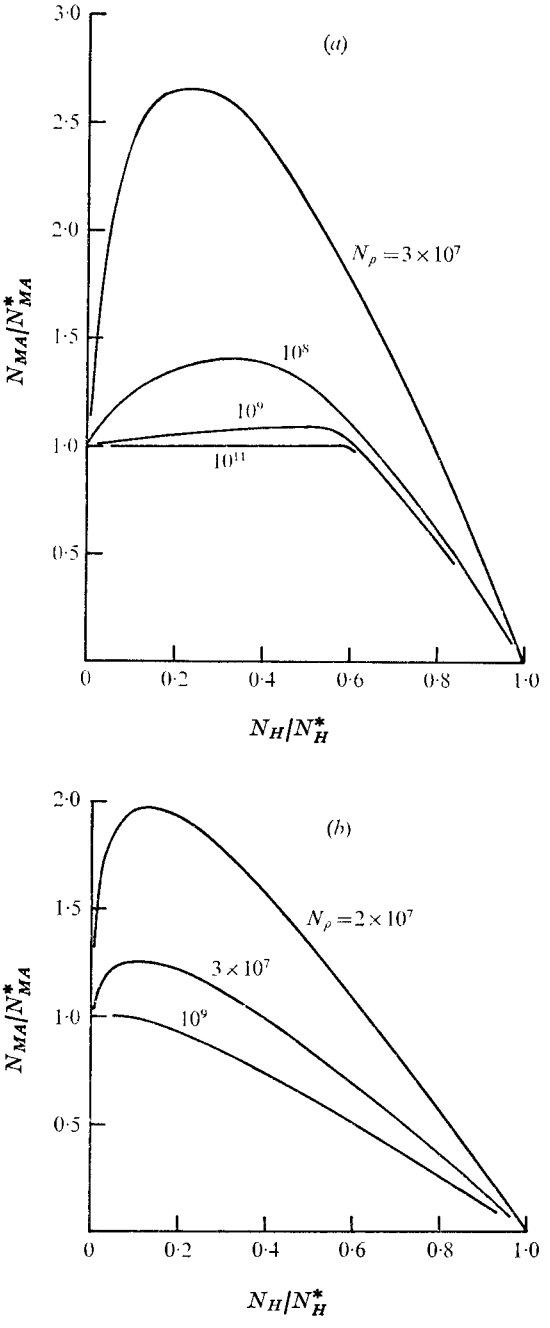

FIGURE 10. The normalized critical Marangoni number *vs.* the normalized critical Hickman number for (*a*) $N_{BO} = 1$ and (*b*) $N_{BO} = 10^{-2}$. $N_{PR} = 10$, $N_{CR} = 10^{-4}$, $N_\mu = 10^2$, $N_{RE} = 10^{-4}$, $N_{BR} = 0$.

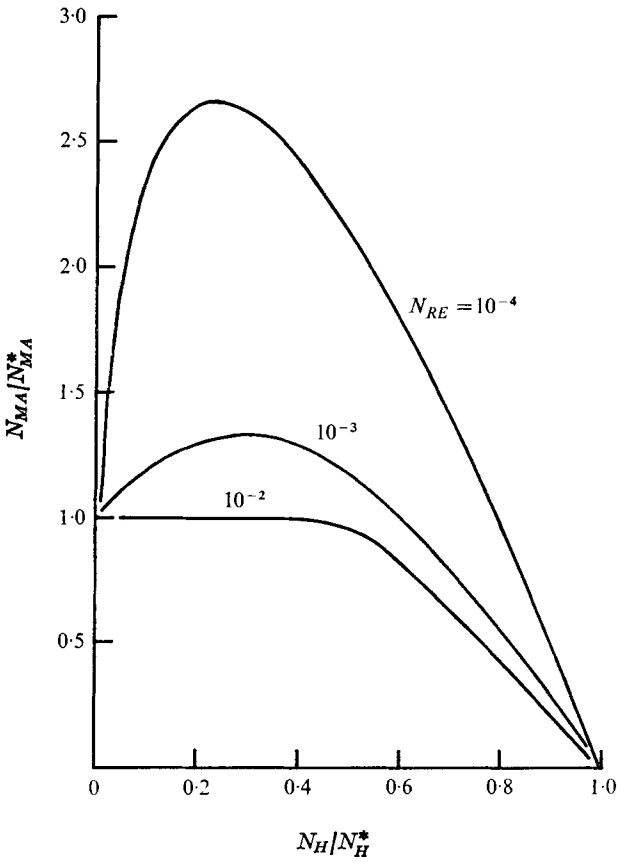

FIGURE 11. The effect of Reynolds number on the coupling between the destabilizing mechanisms of differential vapour recoil and surface tension. $N_{BO} = 1$, $N_{PR} = 10$, $N_{CR} = 10^{-4}$, $N_\mu = 10^2$, $N_\rho = 3 \times 10^7$, $N_{BR} = 0$.

intermediate region of stability is caused by the stabilizing effect of evaporative cooling on instability driven by surface tension and is consistent with experimental observations, which verify that the interface of the rapidly evaporating liquid is noticeably calm just before the onset of instability at low pressure ($\sim$ 0·1 Torr).

The lack of co-operation between these destabilizing mechanisms coincides with a sizeable difference in the preferred wavenumber for each mechanism. The critical wavenumber for instability driven by surface tension at $N_{RE} = 10^{-4}$ is 0·02, while that for instability induced by differential vapour recoil is approximately 1·0 for $N_{BO} = 1{\cdot}0$ and about 0·25 for $N_{BO} = 10^{-2}$. It is evident from a comparison of figures 10(*a*) and (*b*) that the coupling between these mechanisms at a fixed value of N_ρ becomes much greater as the preferred wavenumber for vapour-recoil instability is reduced through a reduction in Bond number. A similar effect is illustrated in figure 11, which shows an increase in coupling between these mechanisms as the Reynolds number increases. Table 1 shows that an increase in N_{RE} increases the preferred wavenumber for instability

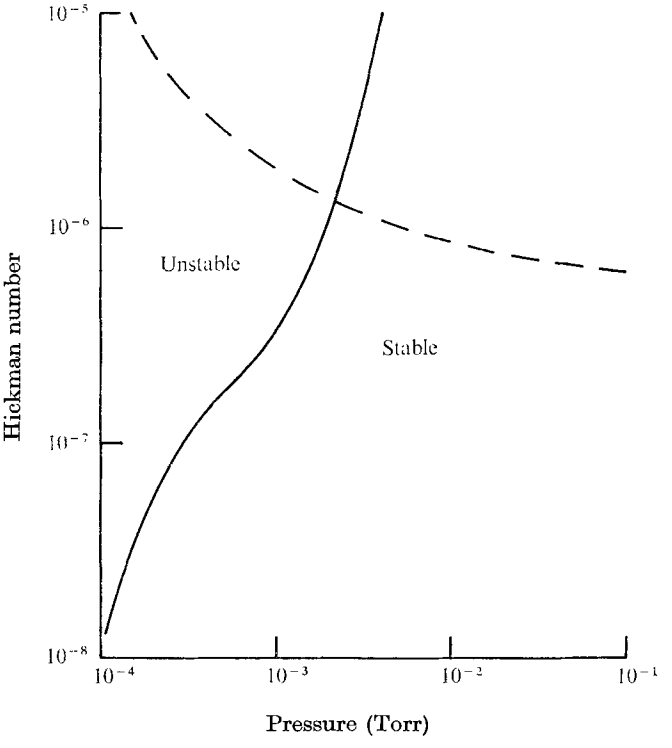

FIGURE 12. Theoretical stability predictions (solid curve) and the experimental trajectory (dashed curve) for steady rapid evaporation of polyphenyl ether at reduced pressures; $\eta^* = 10^{-4}$ g/cm^2 s and $d = 0{\cdot}1$ mm.

driven by surface tension and thereby decreases the degree of competition between the mechanisms.

Although considerable experimental evidence has been compiled by Hickman and myself with regard to trends in the stability behaviour of rapidly evaporating liquids under vacuum, no data exist which precisely identify the criteria for instability in such systems. Nevertheless, the experimental consequences of the theoretical predictions can be explored by considering an experiment similar to those of Hickman (1972) in which polyphenyl ether is evaporated at a steady rate of 10^{-4} g/cm^2 s, sustained by a thermal gradient of 2 °C/cm across a thermal boundary layer 0·1 mm thick. As the pressure above the liquid is gradually reduced, the liquid-to-vapour density ratio increases, significantly reducing the stability limit for the system and increasing the experimental value of the Hickman number. All the other dimensionless groups describing the system are insensitive to pressure and need be computed only once: $N_{PR} = 40$, $N_{CR} = 2 \times 10^{-4}$, $N_{BO} = 5 \times 10^{-3}$, $N_{\mu} = 80$, $N_{RE} = 2{\cdot}5 \times 10^{-5}$, $N_{BR} = 7 \times 10^{-9}$ and $N_{MA} = 4$.

The theoretical criteria for instability induced by differential vapour recoil (solid line) and the associated experimental curve (dashed line) for the above conditions are shown in figure 12. On the basis of these computations, instability should occur at a pressure of about 2×10^{-3} Torr, which is in qualitative agree-

ment with experimental observations. For the above conditions, the critical value of N_H for the viscous-dissipation mechanism may be computed from (40), and is found to be three orders of magnitude greater than the critical N_H for the dominant vapour-recoil mechanism. Similarly, it is easily shown that at such low Reynolds numbers the moving-boundary mechanism is inoperative.

8. Conclusion

The linear stability analysis of a fluid–fluid system undergoing phase transformation reveals that the observed instability during vaporization at reduced pressure can indeed be predicted theoretically. Four distinct destabilizing mechanisms are delineated in the analysis in addition to the familiar surface-tension mechanism. However, computations indicate that under usual circumstances instability is dominated by the destabilizing mechanism of differential vapour recoil. Of particular significance is the competition that exists between the destabilizing surface-tension and vapour-recoil mechanisms to determine the disturbance wavelength which will be most rapidly amplified. The result is that even a pure liquid may proceed from a region of instability driven by surface tension to one exhibiting a torpid (stable) interface to a state in which convection is driven by differential vapour recoil as the evaporation rate is continually increased.

A future paper will be presented to explore the effects of non-volatile surface-active agents on system stability in an attempt to unveil the cause and nature of the schizoid interface.

I thank Kenneth Hickman for the invitation to observe and interpret his experiments on vapour recoil. I also thank William Kayser for thoughtful discussion and criticism and Geraldine Mosholder and Allen Roggen for assistance in the preparation of this manuscript. This work was supported by the Office of Saline Water (now Office of Water Research and Technology) under Grant no. 14-30-3236 and Grant no. 14-30-2964.

REFERENCES

Beitel, A. & Heideger, W. J. 1971 *Chem. Engng Sci.* **26**, 711.
Berg, J. C. 1972 *Recent Developments in Separation*, vol. II, p. 1. C. R. C. Press.
Brian, P. L. T. & Ross, J. R. 1972 *A.I.Ch.E. J.* **18**, 582.
Hickman, K. 1952 *Indust. Engng Chem.* **44**, 1892.
Hickman, K. 1972 *J. Vac. Sci. Tech.* **9**, 960.
McConaghy, G. A. & Finlayson, B. A. 1969 *J. Fluid Mech.* **39**, 49.
Maa, J. R. 1967 *Indust. Engng Chem. Fund.* **6**, 504.
Miller, C. A. 1973 *A.I.Ch.E. J.* **19**, 909.
Nield, D. A. 1964 *J. Fluid Mech.* **19**, 341.
Palmer, H. J. & Berg, J. C. 1972 *J. Fluid Mech.* **51**, 385.
Scriven, L. E. & Sternling, C. V. 1964 *J. Fluid Mech.* **19**, 321.
Slattery, J. C. 1967 *Indust. Engng Chem. Fund.* **6**, 108.
Smith, K. A. 1966 *J. Fluid Mech.* **24**, 401.
Veronis, G. 1965 *J. Mar. Res.* **23**, 1.

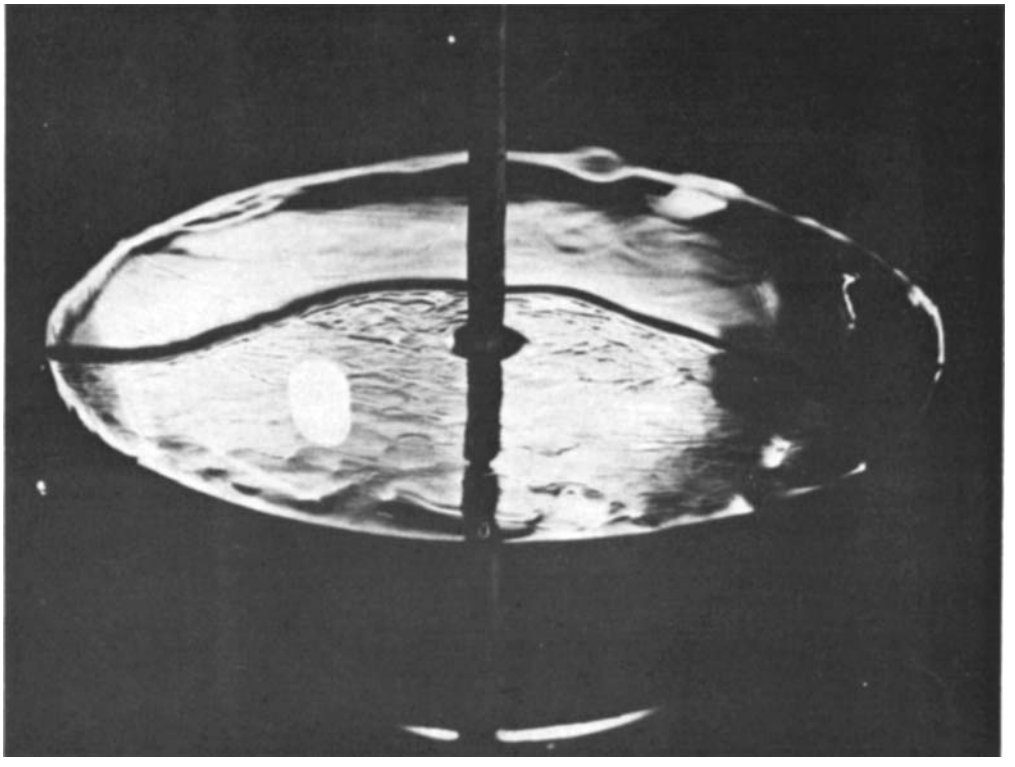

FIGURE 1. The schizoid surface of a rapidly evaporating mineral oil: working area foreground, torpid area behind. (Courtesy of K. Hickman.)